

TCAD for PV: A fast method for accurately modelling metal impurity evolution during solar cell processing

Douglas M. Powell¹, David P. Fenning¹, Jasmin Hofstetter¹, Jean-François Lelièvre², Carlos del Cañizo² & Tonio Buonassisi¹
¹Massachusetts Institute of Technology, Cambridge, Massachusetts, USA; ²Instituto de Energía Solar, Universidad Politécnica de Madrid, Madrid, Spain

Fab & Facilities

Materials

Cell Processing

Thin Film

PV Modules

Power Generation

Market Watch

ABSTRACT

Coupled device and process simulation tools, collectively known as technology computer-aided design (TCAD), have been used in the integrated circuit industry for over 30 years. These tools allow researchers to quickly converge on optimized device designs and manufacturing processes with minimal experimental expenditures. The PV industry has been slower to adopt these tools, but is quickly developing competency in using them. This paper introduces a predictive defect engineering paradigm and simulation tool, while demonstrating its effectiveness at increasing the performance and throughput of current industrial processes. The impurity-to-efficiency (I2E) simulator is a coupled process and device simulation tool that links wafer material purity, processing parameters and cell design to device performance. The tool has been validated with experimental data and used successfully with partners in industry. The simulator has also been deployed in a free web-accessible applet, which is available for use by the industrial and academic communities.

Introduction: why simulate metal impurities?

Computer simulation has transformed industries by allowing rapid, low-cost design iterations during product development. The photovoltaic industry has benefited from device simulators for over 25 years: some early examples include PC1D [1,2], AMPS-1D [3,4], and SCAPS [5,6]. These tools, especially PC1D, continue to have a large influence on the photovoltaics industry. While existing device simulators achieve their intended purpose, an integrated approach that considers the interdependency of processing and performance is superior. Technology computer-aided design (TCAD) tools provide these integrated capabilities. Initial codes were written over 30 years ago and tailored to specific applications in the semiconductor industry [7,8]. The PV industry has lagged behind the integrated circuit industry in the application of process modelling, but interest has recently increased with the availability of commercial packages targeting photovoltaics [9,10]. However, care must be taken when adapting existing tools, designed for the integrated circuit industry, to the PV industry, because of the inherently higher defect densities present in solar-grade silicon material.

The optimization of the time-temperature profile of phosphorus diffusion gettering (PDG) (Fig. 1) presents a useful application of process modelling [11]. In the as-grown wafer, many metal impurities are distributed inhomogeneously as interstitial point defects, found throughout the wafer, and metal-silicide precipitates, found mainly

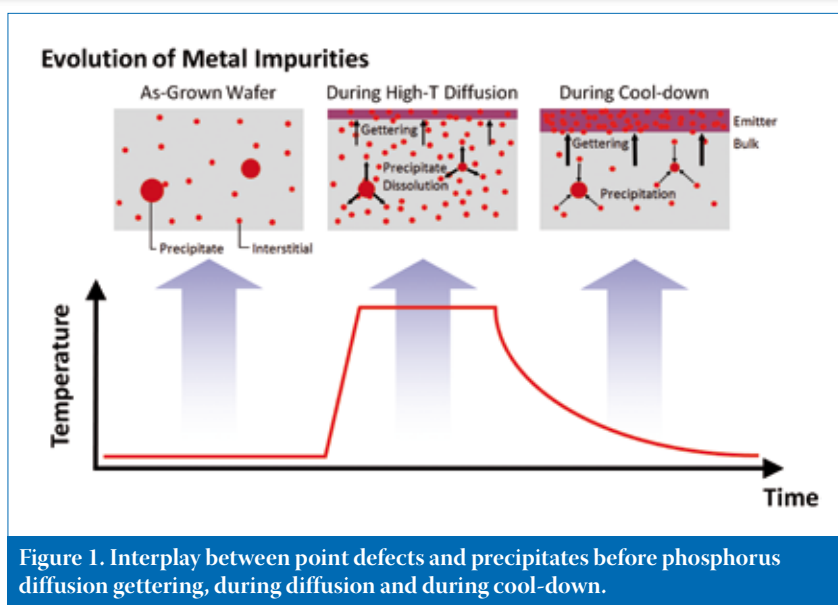


Figure 1. Interplay between point defects and precipitates before phosphorus diffusion gettering, during diffusion and during cool-down.

at structural defects such as dislocations and grain boundaries [12,13]. During the high-temperature plateau and cool-down of PDG, most interstitial metals – e.g. Cu, Fe and Cr – diffuse and segregate to the phosphorus-rich layer, because these species have a higher effective solubility in the *n*-type region than in the *p*-type bulk [14,15]. This decreases the bulk interstitial concentration below the solubility limit at the process temperature, causing metal precipitates to dissolve. The newly dissolved interstitial atoms can then diffuse to the emitter, driving further precipitate dissolution. By the end of the process, PDG generally reduces both total and interstitial metal concentrations and thereby increases cell performance. But the effectiveness of the gettering step critically

depends on the time-temperature profile, and in particular on the cool-down rate, because the segregation coefficient, the ratio of the bulk and emitter solubilities, and the diffusivity of metal point defects are strong functions of temperature.

The PDG process must be optimized to address both the total concentration and the distribution of metal impurities for maximum improvement of minority carrier lifetime [14,16–18]. For example, total as-grown iron concentration is a better predictor of lifetime after gettering than the interstitial as-grown concentration (Fig. 2) [19]. Iron is of particular interest in silicon solar cells because it is typically the performance-limiting defect in as-grown materials [17,20]. Additionally, the concentration

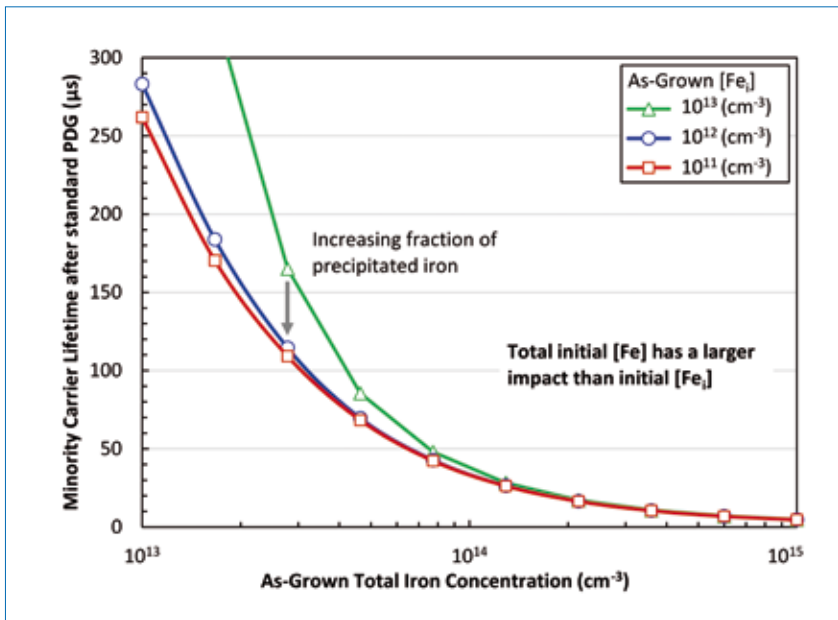


Figure 2. After standard PDG, the bulk lifetime is affected primarily by the as-grown total iron concentration and secondarily by the as-grown interstitial iron concentration. Lifetime calculated with I2E simulation of standard PDG.

of total iron, especially in cast silicon materials, can be orders of magnitude higher than the interstitial iron concentration [21]. The concentration of interstitial iron can be measured with relative ease by flash or thermal dissociation of Fe-B pairs and subsequent re-measurement of the minority carrier lifetime [22]. The total iron concentration, however, including both dissolved and precipitated iron, is more difficult (and costly) to measure, because metal concentrations are often at or below the detection limits of readily available mass-spectroscopy methods.

In a material with high total iron concentrations, for example wafers extracted from the top or borders of an ingot, large metal-silicide precipitates

cannot be completely dissolved in many gettering processes, and act as recombination-active defects and sources of interstitials during subsequent high-temperature processing [23,24]. Additionally, standard gettering processes are less effective in multicrystalline silicon (mc-Si) than in monocrystalline silicon (mono-Si), as dislocations and grain boundaries impede the effective extraction of metal impurities in mc-Si material [25–27]. This contributes to the relatively low efficiencies of mc-Si devices compared to mono-Si [28].

The impurity-to-efficiency (I2E) simulator – a coupled device and process TCAD tool – has been developed to address the challenges of optimizing the time-temperature profile of solar cell

processing to specific distributions and concentrations of iron in as-grown wafers [29]. This paper presents a description of the I2E simulator, a demonstration of the effectiveness of predictive defect engineering in industrial applications, and a discussion of the online implementation of the tool.

“The impurity-to-efficiency (I2E) simulator – a coupled device and process TCAD tool – has been developed to address the challenges of optimizing the time-temperature profile of solar cell processing to specific distributions and concentrations of iron in as-grown wafers.”

Method: predictive defect engineering

The I2E simulation tool has been developed to predict the impact of as-grown iron impurities on final solar cell performance as a function of device processing conditions and cell architecture (Fig. 3) [29]. The I2E simulator operates in 1D to capture the essential physics of iron interstitial gettering and precipitate dissolution with minimum computational expense, and is a compactly packaged deployment of previous simulation efforts [24,30–34]. The simulator consists of three components:

- A kinetic model for the diffusion and segregation of iron point defects, as well as iron-silicide precipitate dissolution and growth, during high-temperature solar cell processing.
- Minority carrier lifetime calculator as a function of both interstitial and precipitated iron concentration using a Shockley-Read-Hall recombination model for the iron interstitial concentration and an effective surface recombination value at iron-silicide precipitate and silicon interfaces.
- The industry standard 1D device simulator, PC1D, to determine device performance as a function of the device architecture, the calculated charge carrier lifetimes and the calculated phosphorus emitter profile [1,2].

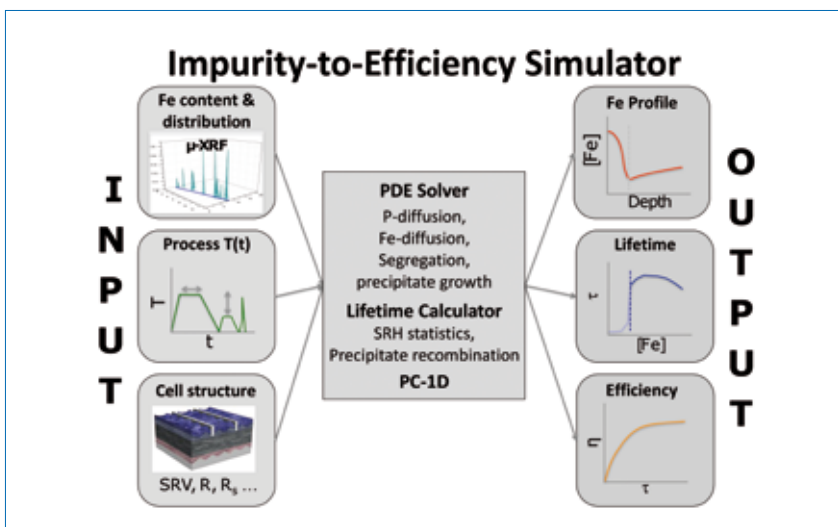


Figure 3. The I2E simulator predicts the impact of as-grown iron impurities on final solar cell performance as a function of device processing conditions and cell architecture.

The kinetic simulator requires the solution of three coupled non-linear partial differential equations [29]. The system of

equations contains steep concentration gradients and fast-moving fronts which are unstable with many numerical methods [35,36]. A solution algorithm was developed that can reliably solve the system of equations and supports the complete dissolution of precipitates. The algorithm generates an optimized spatial mesh distribution for the device. Execution times for practical problems range from 30 seconds to 30 minutes and depend strongly on the resolution of the mesh and complexity of the time-temperature profile. The simulator has been validated through comparisons with experimental data for gettering in mono-Si and mc-Si wafers [29].

Results: improvements guided by predictive defect engineering

The I2E simulator has been successfully employed to optimize cell processing conditions with academic and industrial partners. The success described below demonstrates the potential of predictive defect engineering and the significant performance improvements that can be realized through tailoring processing conditions to specific material qualities.

Process tailoring to specific impurity levels

Approximately half of the wafers produced by ingot casting contain some portion of so-called 'red zones' – regions of low minority carrier lifetime from high residual iron concentrations [37]. A few centimetres of 'red zone' material near the crucible wall are removed from the ingot prior to brick and wafer sawing, as the lifetime typically fails to improve during standard solar cell processing. A low-temperature anneal (LTA) was applied following phosphorus diffusion, to improve the gettering of residual iron. Results of the standard and optimized processes are shown in Fig. 4. Optimized phosphorus diffusion not only improved the minority carrier lifetime over the entire ingot, but also increased the lifetime of the bottom 10% of the ingot to an acceptable value, resulting in a yield increase. In the future, predictive simulation may be employed to optimize solar cell processing for different regions of the ingot, which have specific distributions and concentrations of iron [19].

P-diffusion co-optimization of bulk lifetime and throughput

Cell manufacturers must optimize their manufacturing lines for both device performance and throughput, while accounting for varying impurity levels. Simulations were conducted for an industrial partner to optimize the hold temperature, plateau time and cooling time of a PDG gettering step for both bulk minority carrier lifetime and throughput. Many researchers have found that

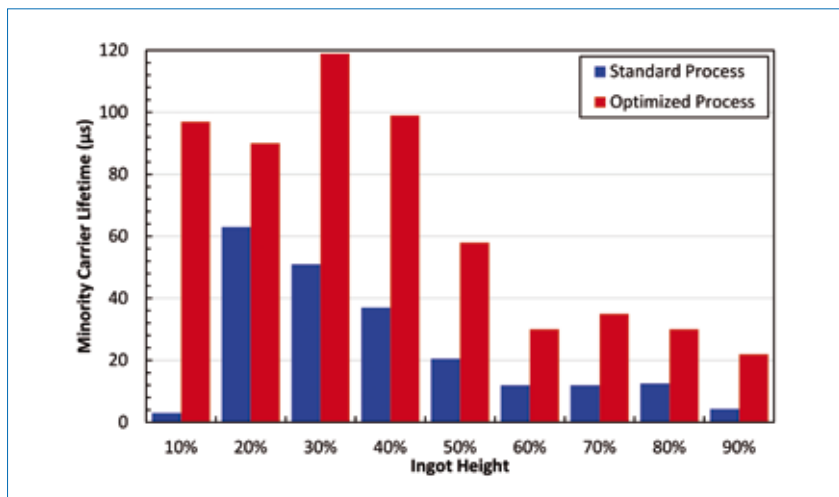


Figure 4. Industrial application: increased ingot yield and material quality through process tailoring to specific impurity levels [38].

extending PDG, by slow cooling or LTA, can improve lifetime by reducing the concentration of interstitial iron [39–44]. More recently, it has been shown that a shorter anneal at lower temperatures can achieve much of the lifetime improvement of extended LTAs by forcing segregation of iron to the external gettering layer [45]. Learning from these previous efforts, in the current study the balance between extending the high-temperature hold time and/or the cooling time was investigated.

I2E simulations were performed to co-optimize lifetime and throughput (Fig. 5). The initial total iron concentration was $3 \cdot 10^{13}$ atoms/cm³, with 10% of the iron present as Fe-B pairs [46] and the remainder homogeneously distributed as 20nm-radius precipitates [23,47]. First, the standard process of our industrial partner was simulated. Next, attempts were made to shorten the standard process while maintaining the existing hold temperature. Although the total

process time was reduced in these cases, the lifetime provided was insufficient for acceptable device performance. Finally, an I2E optimized process was suggested that provided a sufficient bulk minority carrier lifetime for our industrial partner, while doubling throughput.

Reduction in interstitial iron concentration after contact co-firing

To date, significant efforts have been made to optimize the time-temperature profile of PDG to reduce the impact of lifetime-limiting impurities in mc-Si material. In contrast, little attention has been paid to optimizing the time-temperature profile of contact firing in order to control metal impurities, despite it being the final high-temperature step of the solar cell fabrication process and the last opportunity to manipulate the metal impurity distribution. Contact firing is usually carried out at peak temperatures between 800°C and 900°C, and is therefore

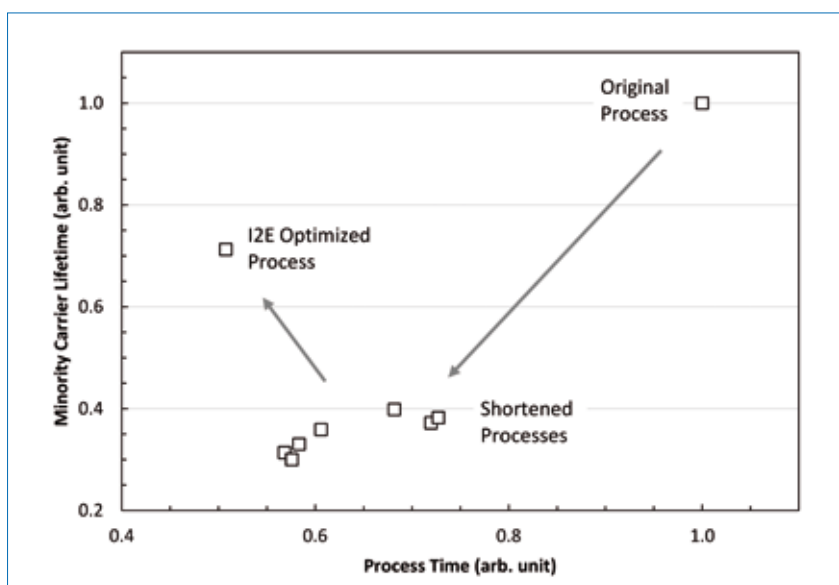


Figure 5. Industrial application: P-diffusion co-optimization of bulk lifetime and throughput.

likely to produce the partial dissolution of metal precipitates, which can offset the reduction in concentration of dissolved impurities achieved during PDG [41,48].

The dissolution and gettering of iron during the co-firing step (Fig. 6) was examined with the I2E simulation tool [49]. First, a standard time-temperature profile of the co-firing step was simulated for a typical iron concentration and distribution in a P-diffused mc-Si wafer. Simulations were carried out for two different peak temperatures, 800°C and 900°C, followed by a rapid cool-down to room temperature. Simulations predict that, after firing at $T_{\text{peak}} = 800^\circ\text{C}$, the interstitial iron concentration remains constant (see blue bars in Fig. 6). After firing at $T_{\text{peak}} = 900^\circ\text{C}$, however, an increased interstitial iron concentration is predicted, indicating that the dissolution of iron precipitates increases at a higher temperature.

“Experimental results confirm that a standard firing step can lead to material degradation, whereas material performance can be maintained or even enhanced during an extended firing step optimized with I2E.”

Second, I2E simulations were performed to optimize the cool-down profile of the firing step to allow for effective gettering of Fe_i atoms to the P-diffused layer. Simulation results suggest that an *extended* firing step, including an additional low-temperature plateau of less than 2 minutes, results in a lower interstitial iron concentration than the standard firing step for both peak

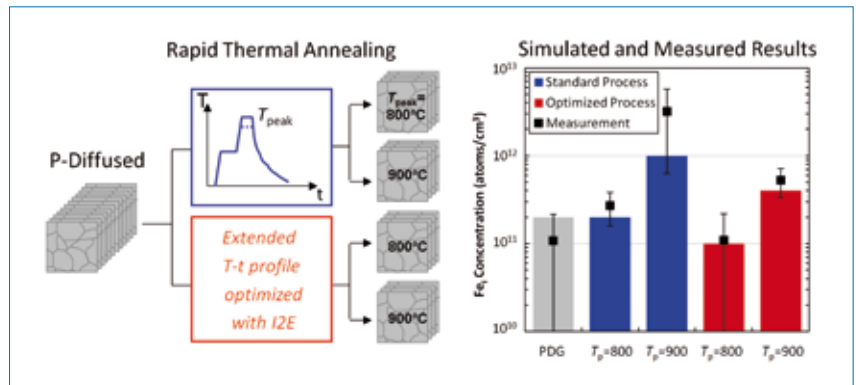


Figure 6. Industrial application: reduction in iron precipitate dissolution during contact co-firing [49].

temperatures (see red bars in Fig. 6). For $T_{\text{peak}} = 800^\circ\text{C}$, an extended firing step can even result in further reduced interstitial iron concentrations after standard PDG.

Simulated trends are confirmed by experimental results, shown as black dots in Fig. 6. Several sets of p-type mc-Si wafers were P-diffused using a standard process, then divided into four groups and subjected to peak temperatures of 800°C or 900°C while following a standard firing or extended firing profile in a rapid thermal annealing (RTA) furnace. Interstitial iron concentrations and electron lifetimes were measured on P-diffused and fired wafers [49]. Experimental results confirm that a standard firing step can lead to material degradation, whereas material performance can be maintained or even enhanced during an extended firing step optimized with I2E.

Discussion: online tool implementation

The simulator has been deployed in a free web-accessible applet [50], which is available for use by the industrial and academic communities. The applet’s user

interface, shown in Fig. 7, allows users to configure simulations and interpret output data. Required inputs to the tool include the time-temperature profile used during cell fabrication, the as-grown total and interstitial iron concentrations in the wafer, and the average precipitate radius. Impurity concentrations can be estimated from the ingot location of the wafer, or measured using a combination of Fe-B dissociation and mass-spectrometry methods such as ICP-MS [51]. Precipitate radius can be estimated as described in the literature [18,23]. Though only needed to simulate device performance, cell architecture is defined by a PC1D parameter (.prm) file.

The applet communicates with a dedicated high-performance server (maintained by the MIT Photovoltaic Research Laboratory in Cambridge) that carries out all calculations all input and output files after results are printed to the user. The applet was initially made available to a user group of approximately 80 individuals. Over 1300 simulations have now been performed during the first three months of operation, with users concentrated in North America, Europe and Asia.

Conclusions

The effectiveness of predictive defect engineering while using the I2E simulation tool has been demonstrated. This tool has benefited the photovoltaic community by providing the information necessary for understanding the interplay between material purity, processing parameters, cell design and device performance. Through the work carried out on this project, it has been concluded that significant performance and throughput improvements can be realized by tailoring processing conditions to specific material qualities. Additionally, the I2E tool allows a rapid optimization of existing processes and the identification and evaluation of new approaches with minimal expenditures. Readers are encouraged to explore problems of interest with the online implementation of the tool.

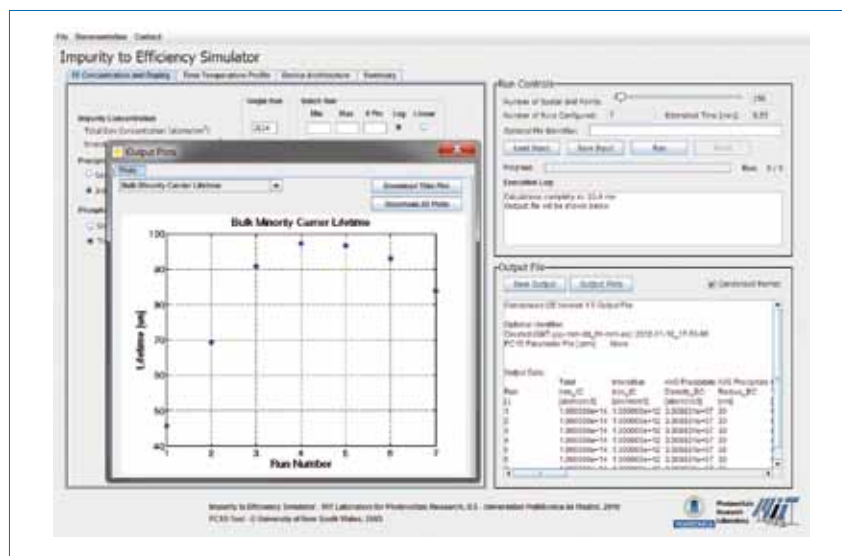


Figure 7. I2E simulator screenshot after calculations are complete: a plot of the results is shown, as well as an output text file.

Acknowledgements

This work was supported by the U.S. Department of Energy (Contract No. DE-FG36-09GO1900), the MIT Deshpande Center, the MIT-Spain/La Cambra de Barcelona Seed Fund and the Spanish Ministerio de Ciencia e Innovación (through Thincells Project No. TEC2008-06798-C03-02). The authors thank N. Stoddard and R. Sidhu, who collaborated in the study leading to the results presented in Fig. 4. In addition, D.M. Powell acknowledges the support of the Department of Defense through the NDSEG fellowship programme, and D.P. Fenning acknowledges the support of the NSF Graduate Research Fellowship.

References

- [1] Clugston, D.A. & Basore, P.A. 1997, "PC1D version 5: 32-bit solar cell modeling on personal computer", *Proc. 26th IEEE PVSC*, Anaheim, California, USA, pp. 207–210.
- [2] Basore, P.A. 1990, "Numerical modeling of textured silicon solar cells using PC-1D", *IEEE Trans. Electron. Dev.*, Vol. 37, No. 2, pp. 337–343.
- [3] Zhu, H. et al. 1999, "Applications of AMPS-1D for solar cell simulation", *Proc. AIP Conf.*, Vol. 462, No. 1, pp. 309–314.
- [4] Fonash, S.J. et al. 1997, "A manual for AMPS-1D for Windows 95/NT".
- [5] Burgelman, M., Nollet, P. & Degraeve, S. 2000, "Modelling polycrystalline semiconductor solar cells", *Thin Solid Films*, Vol. 361–362, pp. 527–532.
- [6] Niemegeers, A. & Burgelman, M. 1996, "Numerical modelling of AC-characteristics of CdTe and CIS solar cells", *Proc. 25th IEEE PVSC*, Washington DC, USA, pp. 901–904.
- [7] Antoniadis, D.A., Hansen, S.E. & Dutton, R.W. 1978, "Supreme II – A program for IC process modeling and simulation", Technical Report No. 5019-2, Stanford Electronics Laboratory.
- [8] Ananthasuresh, G.K. (ed.) 2003, *Optimal Synthesis Methods for MEMS*. Norwell, MA: Kluwer Academic.
- [9] Cowen, N.E.B. & Ahn, C. 2011, "TCAD in the semiconductor industry and its advantages for solar cell manufacturing", *PVI*, 12th edn, pp. 72–80.
- [10] Michael, S. & Michalopoulos, P. 2002, "Application of the SILVACO/ATLAS software package in modeling and optimization of state-of-the-art photovoltaic devices", *Proc. 45th Midwest Symp. Circ. & Syst.*, Washington DC, USA, 651–654.
- [11] Goetzberger, A. & Shockley, W. 1960, "Metal precipitates in silicon p-n junctions", *J. Appl. Phys.*, Vol. 31, pp. 1821–1824.
- [12] Bertoni, M.I. et al. 2011, "Nanoprobe X-ray fluorescence characterization of defects in large-area solar cells", *Energy & Env. Sci.*, Vol. 4, No. 10, pp. 4252–4257.
- [13] Liu, A., Fan, Y.-C. & Macdonald, D. 2011, "Interstitial iron concentrations across multicrystalline silicon wafers via photoluminescence imaging", *Prog. Photovolt: Res. Appl.*, Vol. 19, No. 6, pp. 649–657.
- [14] Kang, J. 1989, "Gettering in silicon", *J. Appl. Phys.*, Vol. 65, No. 8, p. 2974.
- [15] Gilles, D., Schröter, W. & Bergholz, W. 1990, "Impact of the electronic structure on the solubility and diffusion of 3d transition elements in silicon", *Physical Review B*, Vol. 41, No. 9, pp. 5770–5782.
- [16] Hopkins, R.H. & Rohatgi, A. 1986, "Impurity effects in silicon for high efficiency solar cells", *J. Cryst. Growth*, Vol. 75, pp. 67–79.
- [17] Coletti, G. et al. 2011, "Impact of metal contamination in silicon solar cells", *Adv. Functional Mater.*, Vol. 21, pp. 879–890.
- [18] Buonassisi, T. et al. 2005, "Engineering metal-impurity nanodefects for low-cost solar cells", *Nature Mater.*, Vol. 4, pp. 676–679.
- [19] Hofstetter, J. et al. 2011, "Towards the tailoring of P diffusion gettering to as-grown silicon material properties", *Solid State Phenom.*, Vol. 178–179, pp. 158–165.
- [20] Sopori, B.L. 1987, "Crystal defects in RTR ribbons: Their characteristics and influence on the ribbon cell performance", *J. Cryst. Growth*, Vol. 82, pp. 228–236.
- [21] Macdonald, D. et al. 2005, "Transition-metal profiles in a multicrystalline silicon ingot", *J. Appl. Phys.*, Vol. 97, p. 033523.
- [22] Zoth, G. & Bergholz, W. 1990, "A fast, preparation-free method to detect iron in silicon", *J. Appl. Phys.*, Vol. 67, No. 11, pp. 6764–6771.
- [23] Fenning, D.P. et al. 2011, "Iron distribution in silicon after solar cell processing: Synchrotron analysis and predictive modeling", *Appl. Phys. Lett.*, Vol. 98, No. 16, p. 162103.
- [24] Schon, J. et al. 2011, "Understanding the distribution of iron in multicrystalline silicon after emitter formation: Theoretical model and experiments", *J. Appl. Phys.*, Vol. 109, No. 6, p. 063717.
- [25] Sopori, B.L., Jastrzebski, L. & Tan, T. 1996, "A comparison of gettering in single- and multicrystalline silicon for solar cells", *Proc. 25th IEEE PVSC*, Washington DC, USA, pp. 625–628.
- [26] Bentzen, A. et al. 2006, "Gettering of transition metal impurities during phosphorus emitter diffusion in multicrystalline silicon solar cell processing", *J. Appl. Phys.*, Vol. 99, p. 093509.
- [27] Istratov, A.A. et al. 2003, "Metal content of multicrystalline silicon for solar cells and its impact on minority carrier diffusion length", *J. Appl. Phys.*, Vol. 94, No. 10, pp. 6552–6559.
- [28] Green, M.A. et al. 2011, "Solar cell efficiency tables (Version 38)", *Prog. Photovolt: Res. Appl.*, Vol. 19, No. 5, pp. 565–572.
- [29] Hofstetter, J. et al. 2011, "Impurity-to-efficiency simulator: predictive simulation of silicon solar cell performance based on iron content and distribution", *Prog. Photovolt: Res. Appl.*, Vol. 19, No. 4, pp. 487–497.
- [30] Haarahiltunen, A. et al. 2005, "Modeling of heterogeneous precipitation of iron in silicon", *Appl. Phys. Lett.*, Vol. 87, No. 15, p. 151908.
- [31] Smith, A.L., Dunham, S.T. & Kimerling, L.C. 1999, "Transition metal defect behavior and Si density of states in the processing temperature regime", *Physica B: Condensed Matter*, Vol. 273–274, pp. 358–362.
- [32] Cañizo, C. del & Luque, A. 2000, "A comprehensive model for the gettering of lifetime-killing impurities in silicon", *J. Electrochem. Soc.*, Vol. 147, No. 7, pp. 2685–2692.
- [33] Plekhanov, P.S. et al. 1999, "Modeling of gettering of precipitated impurities from Si for carrier lifetime improvement in solar cell applications", *J. Appl. Phys.*, Vol. 86, No. 5, pp. 2453–2458.
- [34] Hieslmair, H. et al. 1998, "Analysis of iron precipitation in silicon as a basis for gettering simulations", *J. Electrochem. Soc.*, Vol. 145, No. 12, pp. 4259–4264.
- [35] Vande Wouwer, A., Saucez, P. & Schiesser, W.E. 2003, "Simulation of distributed parameter systems using a Matlab-based method of lines toolbox: Chemical engineering applications", *Ind. Eng. Chem. Res.*, Vol. 43, No. 14, pp. 3469–3477.
- [36] Ames, W.F. 1992, *Numerical Methods for Partial Differential Equations*. Boston, MA: Academic Press.
- [37] Nærland, T.U., Arnberg, L. & Holt, A. 2009, "Origin of the low carrier lifetime edge zone in multicrystalline PV silicon", *Prog. Photovolt: Res. Appl.*, Vol. 17, No. 5, pp. 289–296.
- [38] Stoddard, N. & Sidhu, R. 2010, "Gettering of impurities in cast monocrystalline silicon", *Proc. MRS Spring Meeting*, San Francisco, California, USA.
- [39] Manshanden, P. & Geerligs, L.J. 2006, "Improved phosphorus gettering of multicrystalline silicon", *Solar Energy*

- Mater. & Solar Cells*, Vol. 90, pp. 998–1012.
- [40] Pickett, M.D. & Buonassisi, T. 2008, “Iron point defect reduction in multicrystalline silicon solar cells”, *Appl. Phys. Lett.*, Vol. 92, p. 122103.
- [41] Tan, J. et al. 2007, “Optimised gettering and hydrogenation of multicrystalline silicon wafers for use in solar cells”, *Proc. 22nd EU PVSEC*, Milan, Italy.
- [42] Hofstetter, J. et al. 2010, “Study of internal versus external gettering of iron during slow cooling processes for silicon solar cell fabrication”, *Solid State Phenom.*, Vol. 156–158, pp. 387–393.
- [43] Härkönen, J. et al. 2003, “Recovery of minority carrier lifetime in low-cost multicrystalline silicon”, *Solar Energy Mater. & Solar Cells*, Vol. 73, pp. 125–130.
- [44] Rinio, M. et al. 2011, “Improvement of multicrystalline silicon solar cells by a low temperature anneal after emitter diffusion”, *Prog. Photovolt: Res. Appl.*, Vol. 19, No. 2, pp. 165–169.
- [45] Hofstetter, J. et al. 2011, “Enhanced iron gettering by short, optimized low-temperature annealing after phosphorus emitter diffusion for industrial silicon solar cell processing”, *physica status solidi (c)*, Vol. 8, No. 3, pp. 759–762.
- [46] Coletti, G. et al. 2008, “Effect of iron in silicon feedstock on p- and n-type multicrystalline silicon solar cells”, *J. Appl. Phys.*, Vol. 104, p. 104913.
- [47] Buonassisi, T. et al. 2005, “Synchrotron-based investigations of the nature and impact of iron contamination in multicrystalline silicon solar cell materials”, *J. Appl. Phys.*, Vol. 97, p. 074901.
- [48] Schön, J. et al. 2010, “2D modelling of the iron concentration from crystallization to final firing of mc silicon solar cells”, *Proc. 25th EU PVSEC*, Valencia, Spain.

- [49] Lelièvre, J.-F. et al. 2011, “Dissolution and gettering of iron during contact co-firing”, *Energy Procedia*, Vol. 8, pp. 257–262.
- [50] Buonassisi Group 2012, Impurity-to-Efficiency Simulator [available online at <http://pv-i2e.mit.edu>].
- [51] Gray, A.L. 1985, “The ICP as an ion source—origins, achievements and prospects”, *Spectrochim. Acta, Part B*, Vol. 40, No. 10–12, pp. 1525–1537.

About the Authors



Douglas M. Powell received a B.S.M.E. from Ohio State University in 2008. After spending some time at GE Wind as a customer value engineer, Douglas is now working towards a Ph.D. in mechanical engineering at MIT. His current research focuses on structural defects in silicon and c-Si PV manufacturing.



David P. Fenning received a B.S. in mechanical engineering from Stanford University in 2008. He is currently studying for a Ph.D. in mechanical engineering at MIT after receiving his M.S. in 2010. David's research interests include impurity kinetics in silicon, defect characterization in semiconductors, and alternative device architectures for improved solar cell efficiency.



Jasmin Hofstetter received a degree in physics from Freie Universität Berlin in Germany in 2006 and completed her Ph.D. in photovoltaic solar energy at Universidad Politécnica de Madrid in Spain. Dr. Hofstetter is currently working as a postdoctoral fellow at MIT, where she is studying the kinetics of metallic impurities and structural defects in silicon, and their interaction during solar cell processing.



Jean-François Lelièvre is an engineer in materials and nanotechnologies (INSA of Rennes) and received his Ph.D. degree in 2007 (INSA of Lyon). After a 2-year postdoctoral appointment at the Instituto de Energía Solar in Madrid, Dr. Lelièvre joined CENTESIL, where he now researches silicon crystallization.



Carlos del Cañizo is an engineer in telecommunications. He received his Ph.D. degree in 2000 and is currently the head of the Instituto de Energía Solar at the Universidad Politécnica de Madrid. Prof. del Cañizo has been involved in the fabrication and characterization of silicon solar cells since 1994, and also works in the area of silicon ultrapurification.



Tonio Buonassisi heads the Photovoltaic Research Laboratory at MIT, which combines crystal growth, processing, characterization, defect simulation and cost-performance modelling to engineer naturally abundant and manufacturable materials into cost-effective, high-performance devices. Prof. Buonassisi's research interests include silicon (thin kerfless absorbers, laser processing, advanced manufacturing), thin films (Earth-abundant chalcogenides and oxides) and high-efficiency concepts.

Enquiries

D. M. Powell
Massachusetts Institute of Technology
Laboratory for Photovoltaic Research
Cambridge, MA 02139
USA

Email: i2e_simulator@mit.edu
Website: <http://pv-i2e.mit.edu/>